



HAL
open science

1-Carbazolyl Spirobifluorene Synthesis, Structural, Electrochemical, and Photophysical Properties

Lambert Sicard, Cassandre Quinton, Fabien Lucas, Olivier Jeannin, Joelle Rault-Berthelot, Cyril Poriel

► **To cite this version:**

Lambert Sicard, Cassandre Quinton, Fabien Lucas, Olivier Jeannin, Joelle Rault-Berthelot, et al.. 1-Carbazolyl Spirobifluorene Synthesis, Structural, Electrochemical, and Photophysical Properties. Journal of Physical Chemistry C, 2019, 123 (31), pp.19094-19104. 10.1021/acs.jpcc.9b02507 . hal-02278422

HAL Id: hal-02278422

<https://univ-rennes.hal.science/hal-02278422>

Submitted on 14 Oct 2019

HAL is a multi-disciplinary open access archive for the deposit and dissemination of scientific research documents, whether they are published or not. The documents may come from teaching and research institutions in France or abroad, or from public or private research centers.

L'archive ouverte pluridisciplinaire **HAL**, est destinée au dépôt et à la diffusion de documents scientifiques de niveau recherche, publiés ou non, émanant des établissements d'enseignement et de recherche français ou étrangers, des laboratoires publics ou privés.

1-Carbazolyl Spirobifluorene: Synthesis, Structural, Electrochemical and Photophysical Properties

Lambert Sicard, Cassandre Quinton, Fabien Lucas, Olivier Jeannin, Joëlle Rault-Berthelot, and Cyril Poriel*

Univ Rennes, CNRS, ISCR-UMR 6226, F-35000 Rennes, France

Abstract

The present work reports one of the rare examples of a new emerging family of spirobifluorene derivatives, namely 1-substituted spirobifluorenes. We report the synthesis and the structural, electrochemical and photophysical properties of 9-(9,9'-spirobifluorene-1-yl)-9H-carbazole **1-Cbz-SBF**, constructed from the connection of the widely known electron-rich carbazole fragment at the C1 position of spirobifluorene. We show with **1-Cbz-SBF** that the substitution at C1 induces two important characteristics which drive the electronic properties. First, there is a complete π -conjugation breaking between the pending substituent, herein carbazole, and the substituted fluorene. Second, there is a through space interaction between the carbazole and its cofacial fluorene. Thanks to a structure-property relationship approach with its constituting building blocks 9,9'-spirobifluorene **SBF** and carbazole **Cbz**, we show how some electronic properties are driven by the carbazole unit such as the HOMO energy level whereas others are driven by the fluorene such as the triplet state energy level. As 1-substituted spirobifluorenyl represents a new and promising molecular scaffold for PhOLED applications and more generally for organic electronics, such study provides fundamental knowledge to design future organic materials for specific applications.

Introduction

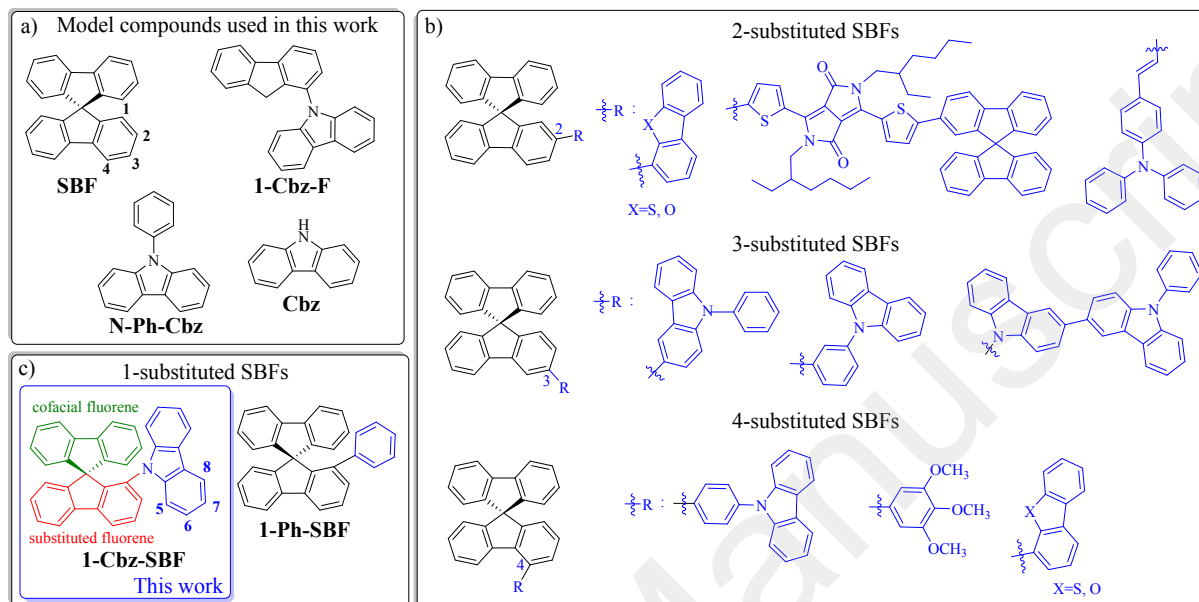
9,9'-Spirobifluorene (SBF) is one of the most important building block used in the synthesis of Organic Semi-Conductors (OSCs) for Organic Electronics (OE).¹⁻⁵ In recent years, manipulating the substitution pattern of SBF has appeared as a very efficient tool to tune the electronic properties of SBF-based materials.^{1-2, 6} In the SBF fragment, there are four positions available for the substitution of each phenyl units numbered 1 to 4 (Chart 1a). This substitution pattern drives the electronic properties of SBF compounds. The position C2 forms a *para*-substituted biphenyl and has significantly contributed to the development of highly efficient SBF-based materials for OE (chart 1b), mainly as emitters in blue Organic Light-Emitting Diodes (OLEDs)^{3, 5, 7-12} but also as electron¹³ or hole¹⁴ transporters in OLEDs and even more recently as very efficient three-dimensional non-fullerene acceptors in organic solar cells.¹⁵⁻¹⁹ The three other positions of the SBF fragment have been far less described to date but appear nevertheless highly promising to build new OSCs.^{1, 20-22} The first examples of SBF-based materials substituted at C4 (*ortho*-substituted biphenyl)²¹ and at C3 (*meta*-substituted biphenyl)²² have only been described in the last ten years, in 2009 and 2013 respectively. The substitution at C1 (*meta* biphenyl linkage) has only been

1
2
3 reported in 2017.¹ However, and oppositely to the substitution at C2, the particularity of the
4 substitution at C1, C3 or C4 is the restriction of the electronic coupling between the fluorene unit
5 and the attached substituent. This key characteristic has been advantageously used to design high
6 triplet energy materials ($E_T > 2.7$ eV), which are particularly attractive for hosting phosphors in
7 Phosphorescent OLED (PhOLEDs).^{2,20} Thanks to the combination of a strong steric hindrance and
8 an electronic decoupling, 1-substituted SBF scaffold seems to be the most efficient regioisomer to
9 construct high E_T materials (for example, **1-Ph-SBF** (chart 1c) possesses an E_T of 2.86 eV).¹
10 On the other hand, it is widely known when designing OSCs for organic electronics that the
11 incorporation of electron-withdrawing and/or electron donating units is an efficient strategy to
12 modulate electronic properties with the aim of reaching high-performance devices. However, it
13 has been shown that the impact of these electron-rich (-poor) functional units is very different as
14 a function of the SBF isomer involved.^{2, 6, 23-24} Indeed, the electronic coupling between the pending
15 substituent and the fluorene unit depends on the SBF substitution pattern and the resulting steric
16 hindrance and/or nature of the linkage (*ortho*, *meta*, *para*). For example, it has been shown that
17 the modulation of HOMO and LUMO energy levels is very different for 2- and 4-substituted
18 SBFs.^{18,19} Thus, in order to increase the molecular diversity of the emerging family of 1-substituted
19 SBFs and to apprehend its electronic properties, we report herein the first example of a 1-
20 substituted SBF incorporating an electron-rich fragment, namely the widely known carbazole unit.
21 The present work reports a detailed structure-property relationship study of 1-carbazolyl-
22 spirobifluorene (**1-Cbz-SBF**) in regard of its constituting building blocks (Spirobifluorene, **SBF**,
23 and carbazole, **Cbz**) and structurally related analogues (1-phenyl-spirobifluorene, **1-Ph-SBF**, 1-
24 carbazolyl-fluorene, **1-Cbz-F** and N-phenyl carbazole **N-Ph-Cbz**). We show how some electronic
25 properties are driven by the carbazole unit such as the HOMO energy level whereas others such as
26 the triplet state energy level E_T are driven by the fluorene. This feature provides an interesting
27 degree of tuning for this family of OSCs.
28
29
30
31
32
33
34
35
36
37

38 Experimental section

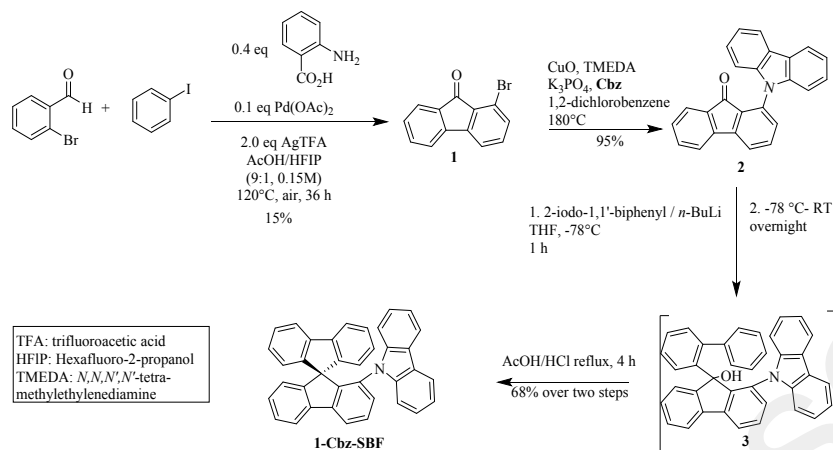
39 Experimental section, synthetic procedures and compounds characterization,
40 structural/electrochemical/photophysical properties, computational details and NMR studies are
41 provided in the Supporting Information.
42
43
44
45
46
47
48
49
50
51
52
53
54
55
56
57
58
59
60

Chart 1. a) Model compounds used in this study and numbering of the substitution position on one phenyl of the SBF unit, b) Examples of SBF positional isomers incorporating electron rich fragments: 2-substituted SBFs,²⁵⁻²⁸ 3-substituted SBFs²⁹⁻³⁰ and 4-substituted SBFs.^{6, 26-27} c) 1-substituted SBFs: **1-Cbz-SBF** and **1-Ph-SBF**¹



Results and discussions

Synthesis. Despite initially developed in 1951,³¹ 1-halogeno-fluorenones have encountered in the last years intense synthetic investigations.^{1, 32-34} These key compounds can be advantageously used in the synthesis of 1-substituted-SBFs as recently shown with **1-Ph-SBF**.¹ In this previous work, a synthetic approach towards 1-iodofluorenone was reported, which has nevertheless the disadvantage of being non-regioselective, also providing 3-iodofluorenone. In the present work, the regioselective one-pot approach towards 1-bromofluorenone **1**, introduced in 2017 by Sorensen and coworkers,³³ has been used (Scheme 1). This reaction is a Pd(II)-catalysed C(sp²) functionalization cascade starting from iodobenzene and 2-bromobenzaldehyde. This one pot approach is not only regioselective but also quick and easy to perform, which should allow to deeply develop 1-fluorenones and consequently 1-substituted SBFs in the future. With **1** in hand, the carbazole fragment was then attached *via* a copper-catalysed Goldberg reaction (CuO/TMEDA/K₃PO₄, 180°C) to provide the corresponding 1-carbazolyl-fluorenone **2** with a high yield of 95%. The synthesis of **1-Cbz-SBF** was then carried out through a classical two-step procedure: lithium-iodine exchange of 2-iodobiphenyl with *n*-butyllithium at low temperature, followed by trapping of the lithiated intermediate with fluorenone **2**. The resulting fluorenol **3** (not isolated) is finally involved in an intramolecular aromatic electrophilic substitution (AcOH/HCl) to provide the 1-carbazolyl-spirobifluorene **1-Cbz-SBF** with a yield of 68% over the two steps. We should mention that, despite a sterically hindered environment, the C1 position allows to incorporate substituents and even a spirolinked fluorene with good yields. Note that 1-carbazolyl-fluorenone **2** can be a useful synthetic intermediate to further introduce other spirolinked fragments of interest for OE such as phenylacridine,³⁵ xanthene,³⁶ or quinolinophenothiazine.³⁷

Scheme 1. Synthesis of 1-carbazolyl-spirobifluorene 1-Cbz-SBF

An important and characteristic in 1-substituted SBFs is the particular face to face arrangement of the pending substituent (colored in blue in chart 1c) and the non-substituted cofacial fluorene (colored in green in chart 1c). Such an arrangement appears unique in the SBF family and the possible interactions between these two fragments have therefore never been studied to date. In order to determine the impact of this cofacial arrangement on the hydrogen atoms resonances, complete ^1H NMR assignments were performed by 2D NMR spectroscopy for **1-Cbz-SBF** and compared to relevant model compounds **SBF**, **1-Ph-SBF** and **Cbz** (Figure 1). All the chemical shifts are gathered in Table S1.

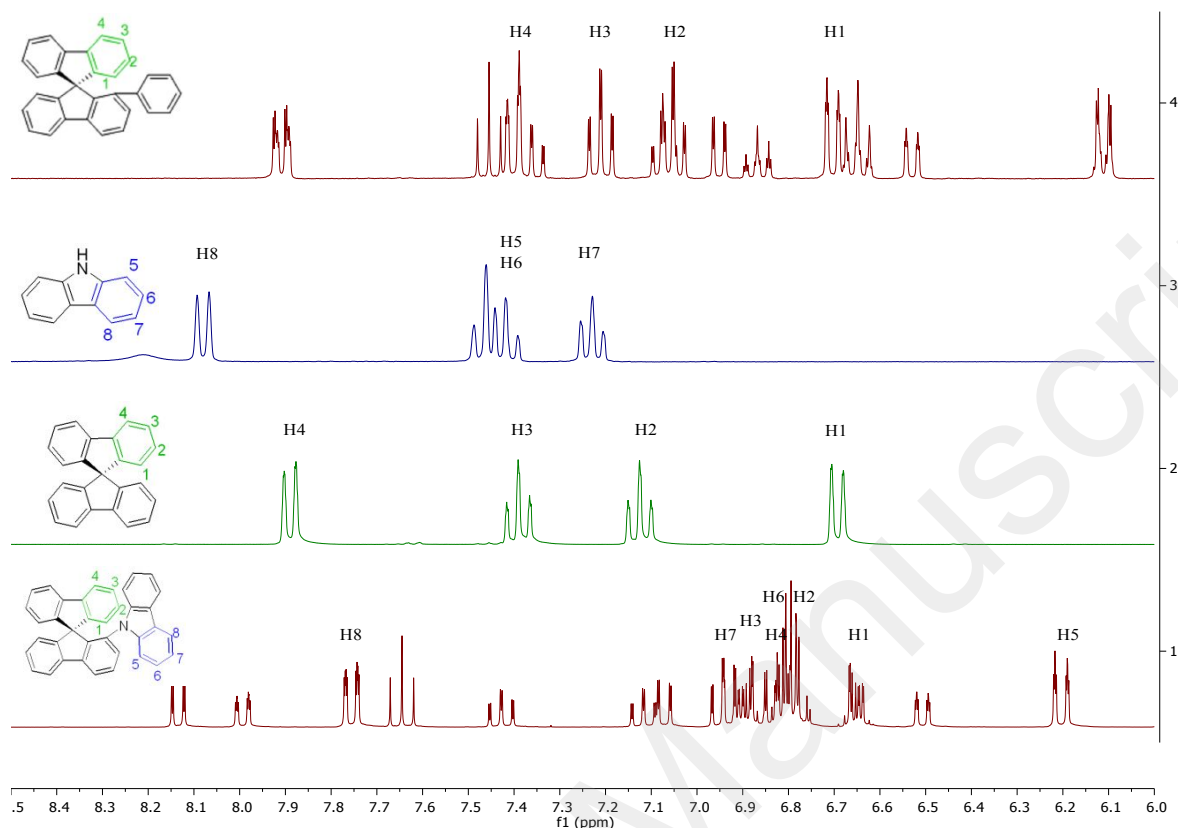


Figure 1. ¹H NMR spectra in CD₂Cl₂ of **1-Ph-SBF**, **Cbz**, **SBF** and **1-Cbz-SBF** (From top to bottom respectively).

In the model compound **SBF**, the chemical shifts of H1-H4 are respectively detected at 6.68, 7.13, 7.39 and 7.89 ppm (Figure 1).³⁸ In **1-Ph-SBF**, H1 is detected at 6.70 ppm, at an almost identical chemical shift than that of **SBF** ($\delta = 6.68$ ppm, Table S1), this proton being therefore not influenced by the cofacial phenyl. On the other hand, H4 is significantly shielded by ca 0.5 ppm in **1-Ph-SBF** compared to its homologue in **SBF** (7.40 vs 7.89 ppm, Figure 1). One can note that the chemical shift difference between the fluorene hydrogen atoms of **SBF** and those of **1-Ph-SBF** gradually increases from H1 to H4. This shielding effect may be assigned to the increased overlap of the two face-to-face aromatic rings of **1-Ph-SBF**. Indeed, transannular π - π interactions are usually accompanied by high field shifts in ¹H NMR spectra and have been observed in many different π -systems such as fluorene,³⁹⁻⁴¹ paracyclophane,⁴² thiophene,⁴³ pyrenes,⁴⁴ and dihydroindeno[2,1-*a*]fluorene.^{5, 38, 41, 45} In the present **1-Cbz-SBF**, the shielding effect is even accentuated compared to **1-Ph-SBF**. Indeed, H1-H4 are respectively detected at 6.65, 6.79, 6.90 and 6.80 ppm, the latter being impressively shielded by more than 1 ppm compared to **SBF** ($\delta = 7.89$ ppm). Thus, due to the inclination of the carbazole unit (see X-ray structure in Figure 2), H4 is the most influenced by the anisotropy cone and hence the most shielded. As a function of the substituent grafted at C1, the chemical shifts of the cofacial fluorene (and hence the strength of the π - π interactions) can be therefore modulated. This is an interesting characteristic of 1-substituted SBFs. The hydrogen atoms of the carbazole unit are also strongly affected by the cofacial arrangement. Indeed, the comparison of the chemical shifts of the hydrogen atoms of the carbazole unit in **1-Cbz-SBF** and in **Cbz** clearly leads to the same conclusions. Thus, hydrogen atoms H5-H8 in **Cbz** are respectively

1
2
3 detected at 7.42, 7.42, 7.21 and 8.06 ppm and at 6.20, 6.83, 6.94 and 7.75 ppm in **1-Cbz-SBF**. In
4 this case, the most influenced hydrogen is H5 in accordance with the inclination of the carbazole
5 unit.
6

7
8 **Structural properties.** Single crystals of **1-Cbz-SBF** were grown from $\text{CHCl}_3/\text{MeOH}$. The first
9 and evident structural particularity of **1-Cbz-SBF** is the cofacial arrangement between the
10 carbazole and the cofacial fluorene. Thanks to the substitution at C1, one can note a very high
11 dihedral angle of 84.1° between the mean plane of the substituted fluorene and that of the
12 carbazole. This large dihedral angle is at the origin of the electronic decoupling noticed below in
13 the physico-chemical properties. In addition, one can note that this angle is higher than that
14 reported for **1-Ph-SBF** (75.4°)¹ and highlights the importance of the substituent itself and
15 especially its size on the structural characteristics. As previously shown for 4-substituted SBFs,^{2,}
16 ²¹ this dihedral angle can be therefore used to modulate the electronic coupling between the
17 fluorene and the pending substituent. The molecular structure of **1-Cbz-SBF** displays many short
18 intramolecular distances between the two cofacial fragments (Figure 2a and Figures S3-S7). Some
19 C/C distances are shorter than the sum of their van der Waals radii (3.4 \AA)⁴⁶ and translate a
20 sterically hindered environment. The shortest distance is measured between the two carbon atoms
21 C1 of the cofacial fluorene and C5 of the carbazole (3.27 \AA). In order to precisely evaluate the
22 strength of these interactions between the carbazole and the cofacial fluorene, three structural
23 parameters have been evaluated for the four cofacial phenyl rings, namely ring-centroid/ring-
24 centroid distance $d_{\text{C-C}}$, vertical displacements d_1 and d_2 and slippage angles θ_1 and θ_2 (Figure 2d
25 and Figure S1 for definitions and calculation methods). As discussed by Janiak and coworkers,
26 these three parameters can reflect the strength of the interactions between two phenyl rings.⁴⁷⁻⁵⁰ In
27 **1-Cbz-SBF**, the ring-centroid/ring-centroid distances between two cofacial phenyl rings of the
28 carbazole and fluorene units are estimated at ca. 3.78 \AA and 3.84 \AA (Figure S2 and Table S2). The
29 smallest vertical displacements between two phenyl rings are very short (0.65 \AA and 0.39 \AA , Table
30 S2) and their corresponding ring slippage angles are very low (9.9° and 5.9° , Table S2). In the
31 light of Janiak's works such values of ring-centroid/ring-centroid distance ($<3.8 \text{ \AA}$), vertical
32 displacements ($<1.5 \text{ \AA}$), and ring slippage angles ($<25^\circ$) indicate strong interactions between
33 carbazole and fluorene.
34
35
36
37
38
39
40
41
42
43
44
45
46
47
48
49
50
51
52
53
54
55
56
57
58
59
60

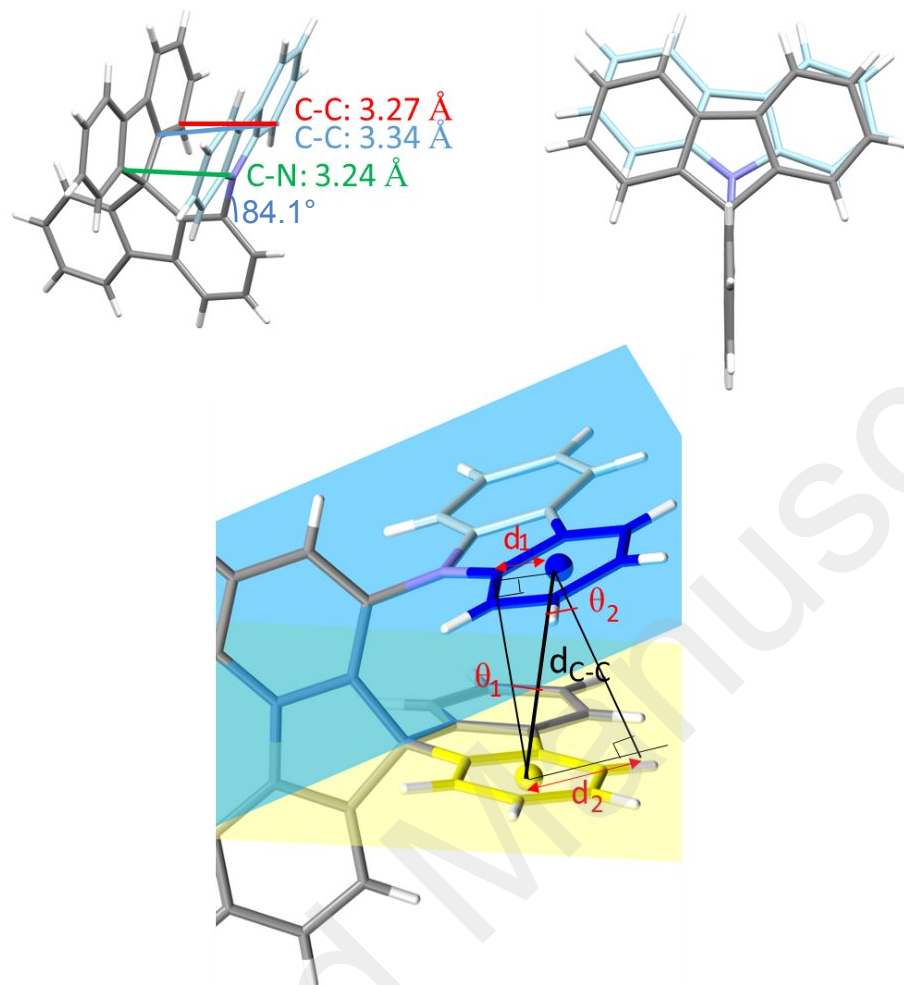


Figure 2. Top) Molecular structure of **1-Cbz-SBF** from X-ray diffraction (two different views) Bottom) Representation of the crystallographic parameters to evaluate the strength of π - π interactions as described by Janiak and coworkers.⁴⁷⁻⁵⁰

Electrochemistry. The electrochemical properties of **1-Cbz-SBF** have been studied in CH_2Cl_2 + Bu_4NPF_6 0.2 M using cyclic voltammetry (CV) and first compared to those of the two constituting building blocks, **Cbz** and **SBF**.

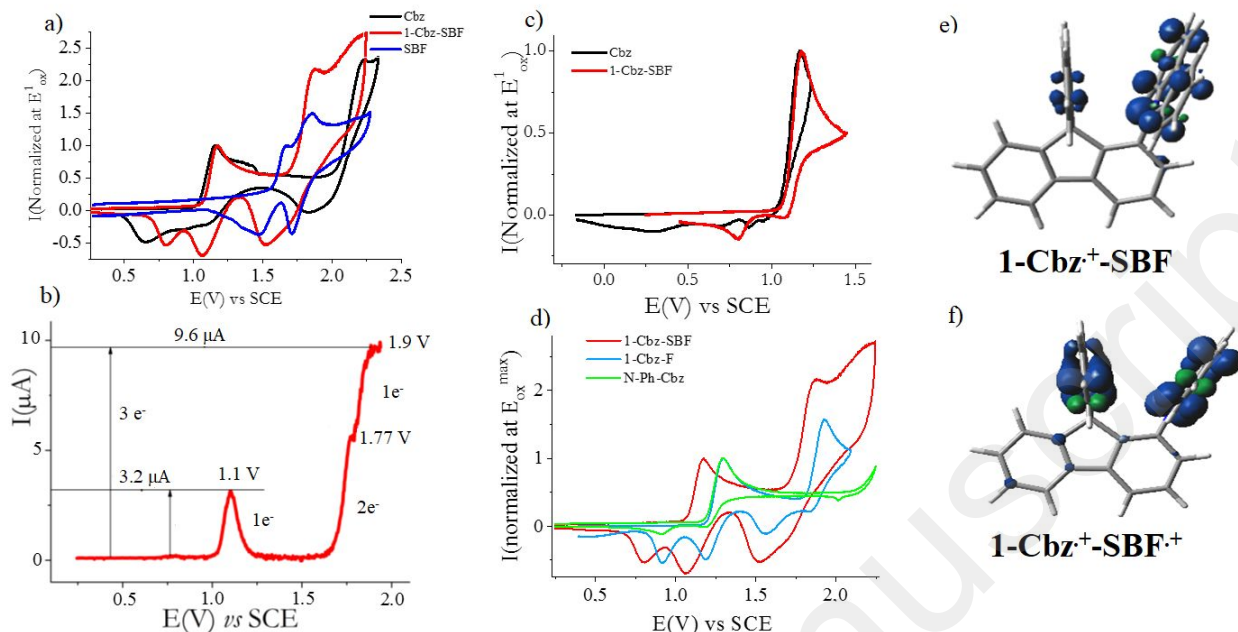


Figure 3. a) CVs recorded at 100 mV s^{-1} (potential range of 0.2/2.2 V) in $\text{CH}_2\text{Cl}_2/[\text{Bu}_4\text{N}][\text{PF}_6]$ 0.2 M in the presence of **1-Cbz-SBF** (red line), **SBF** (blue line), and **Cbz** (black line). b) Differential pulse voltammetry of **1-Cbz-SBF**. c) CVs recorded at 100 mV s^{-1} (potential range of -0.2/1.45 V) in $\text{CH}_2\text{Cl}_2/[\text{Bu}_4\text{N}][\text{PF}_6]$ 0.2 M in the presence of **1-Cbz-SBF** (red line) and **Cbz** (black line). d) CVs recorded at 100 mV s^{-1} (potential range of 0.2/2.25 V) in $\text{CH}_2\text{Cl}_2/[\text{Bu}_4\text{N}][\text{PF}_6]$ 0.2 M in the presence of **1-Cbz-SBF** (red line), **N-Ph-Cbz** (green line) and **1-Cbz-F** (sky blue line). Intensity is normalized at E_{ox}^1 for all the compounds. Spin densities of (e) the cation radical and the bis radical cation (f) of **1-Cbz-SBF** (isovalue = 0.004, cam-b3lyp/6-31g(d)).

In oxidation, **1-Cbz-SBF** presents two distinct waves with maxima at 1.17 and 1.87 V (Figure 3a, red line) followed by an additional oxidation at a potential higher than 2.25 V (potential limit reached). Thus, the first oxidation of **1-Cbz-SBF** occurs at almost identical potential value than that of **Cbz** (1.16 V, Figure 3c, black line) translating an electron transfer centered on the carbazole unit. This is in accordance with the HOMO distribution of **1-Cbz-SBF** (Figure 7) and of the spin density of its cation-radical (Figure 3e) both localized on the carbazole unit. From the onset potential of the first oxidation wave, 1.07 V, the HOMO energy level of **1-Cbz-SBF** is evaluated at -5.47 eV. As HOMO level of **1-Cbz-SBF** is distributed on the carbazole unit, its energy is higher than that of **SBF** (-5.95 eV, HOMO localized on fluorene) and almost identical to that of **Cbz** (-5.50 eV).

At this stage, it is interesting to compare the oxidation of **1-Cbz-SBF** to that of another model compound, N-phenyl-Carbazole (**N-Ph-Cbz**),⁶ the carbazole having a phenyl group substituting the nitrogen atom (See structure in chart 1a). Thus, as presented Figure 3d (green line), the first oxidation of **N-Ph-Cbz** is shifted to more anodic values (1.30 V) compared to that of both **1-Cbz-SBF** and **Cbz** (1.17 V), all CVs being recorded in identical conditions ($\text{CH}_2\text{Cl}_2/[\text{Bu}_4\text{N}][\text{PF}_6]$ 0.2 M). The potential difference between **Cbz** and **N-Ph-Cbz** can be explained by the negative inductive effect of the phenyl ring which leads to a carbazole unit more difficult to oxidize in **N-Ph-Cbz** than in **Cbz**. It is indeed known that the substituent borne by the nitrogen atom has a consequent impact on the first oxidation potential of the carbazole core.⁵¹ For example with a

1
2
3 methyl or an ethyl group borne by the nitrogen atom, the oxidation of the carbazole unit is shifted
4 to lower potentials.⁵¹ It should be specified that, with high dihedral angles of ca 50° reported for
5 different molecules possessing the N-phenyl-carbazole fragment,^{30, 52} there is no or only a very
6 weak electronic coupling between the carbazole and the phenyl (no conjugation extension). As **1-**
7 **Cbz-SBF** is also built with a N-phenyl-carbazole fragment, the anodic shift between **1-Cbz-SBF**
8 and **N-Ph-Cbz** cannot be explained by simple inductive effects and another effect should be
9 invoked. We have shown above that the position of the carbazole at C1 of the SBF core induces a
10 strong interaction with the cofacial fluorene. It is known in literature that the oxidation of π -stacked
11 systems is more facile than their non-stacked analogues.^{39, 53} In the case of fluorenes based systems,
12 several examples have been provided by Rathore and coworkers^{39, 54} or by us.^{38, 41, 55} In the present
13 case, the strong interaction between the cofacial fluorene and the carbazole fragment can be
14 responsible of the shift observed between **1-Cbz-SBF** and **N-Ph-Cbz**. To confirm this hypothesis,
15 another model compound, 1-carbazolylfluorene **1-Cbz-F**, has been synthesized and studied (See
16 structure in chart 1a). In this molecule, there is the same *N*-carbazole-1-fluorene fragment but
17 without any cofacial fluorene. Studying this compound should highlight the through-space
18 interaction in **1-Cbz-SBF**. The first oxidation wave of **1-Cbz-F** displays a maximum at 1.3 V
19 (Figure 3d, sky blue line) shifted by 0.13 V compared to that of **1-Cbz-SBF** (1.17 V). This shift
20 clearly confirms that the π - π intramolecular interactions between the carbazole and its facing
21 fluorene are at the origin of the shift to less positive values of the first oxidation potential in **1-**
22 **Cbz-SBF** (1.17 V). This strategy could be advantageously used to finely tune the first oxidation
23 potential (and hence the HOMO energy level) of 1-substituted SBF based materials. Note that the
24 first oxidation waves of **1-Cbz-F** and **N-Ph-SBF** are both detected at a very similar potential,
25 showing the similar impact of a fluorene or a phenyl ring on the oxidation of these compounds.
26
27
28
29
30

31 For both **1-Cbz-SBF** and **Cbz**, the first oxidation is irreversible showing the high reactivity of the
32 charged species (Figure 3c). The weak reduction waves recorded at the reverse scan for both
33 compounds may be assigned to the reduction of a small amount of oligomers precipitated on the
34 electrode surface during the former oxidation. However, as no new oxidation wave appears on the
35 CV upon successive cycles, one may conclude that these species are soluble in solution in these
36 experimental conditions.
37

38
39 The second oxidation of **1-Cbz-SBF**, with its maximum at 1.87 V, appears more difficult to assign
40 with confidence. As shown by the differential pulse voltammetry (Figure 3b), three electrons are
41 involved in this second oxidation process. As this oxidation occurs in the potential range of the
42 two successive oxidation waves of **SBF** (1.67 & 1.86 V, Figure 3a) two of these electron may be
43 therefore ascribed to the oxidation of the SBF unit. This is in agreement with molecular modelling
44 which shows that the electron density of **1-Cbz-SBF** bis radical cation is spread out on both
45 cofacial fluorene and carbazole (Figure 3f), indicating that the second oxidation involves the
46 cofacial fluorene leading to **1-Cbz⁺-SBF⁺**. The following oxidation processes are nevertheless
47 difficult to modelize because of polymerization.
48
49

50 Another interesting feature related to the oxidation of **1-Cbz-SBF** is the electrodeposition process
51 observed during recurrent cycles when cycling up to or over the second oxidation potential. It is
52 indeed widely known that SBF derivatives can be polymerized by anodic oxidation leading to 3D
53 materials.⁵⁶⁻⁶⁰ However, anodic polymerization of 1-substituted SBFs has never been reported to
54 date. As presented Figure 4-left, one observes the appearance and the regular growth of three new
55
56
57
58
59
60

redox waves centered at 0.90, 1.20 and 1.60 V when cycling up to 1.80 V or at 1.00, 1.30 and 1.80 V when cycling up to 2.25 V.

Depending on the anodic limit, the intensity of the new waves increases in a different manner. When cycling to 1.80 V, the currents measured after ten cycles are ca 2 to 3 times higher than those measured at the first cycle. However, when cycling to 2.25 V, the three waves increase more intensively (ca 7 times). This feature can be assigned to the number of positions involved in the electrodeposition process (mainly carbazole units in the first case and both carbazole and fluorene units in the second).

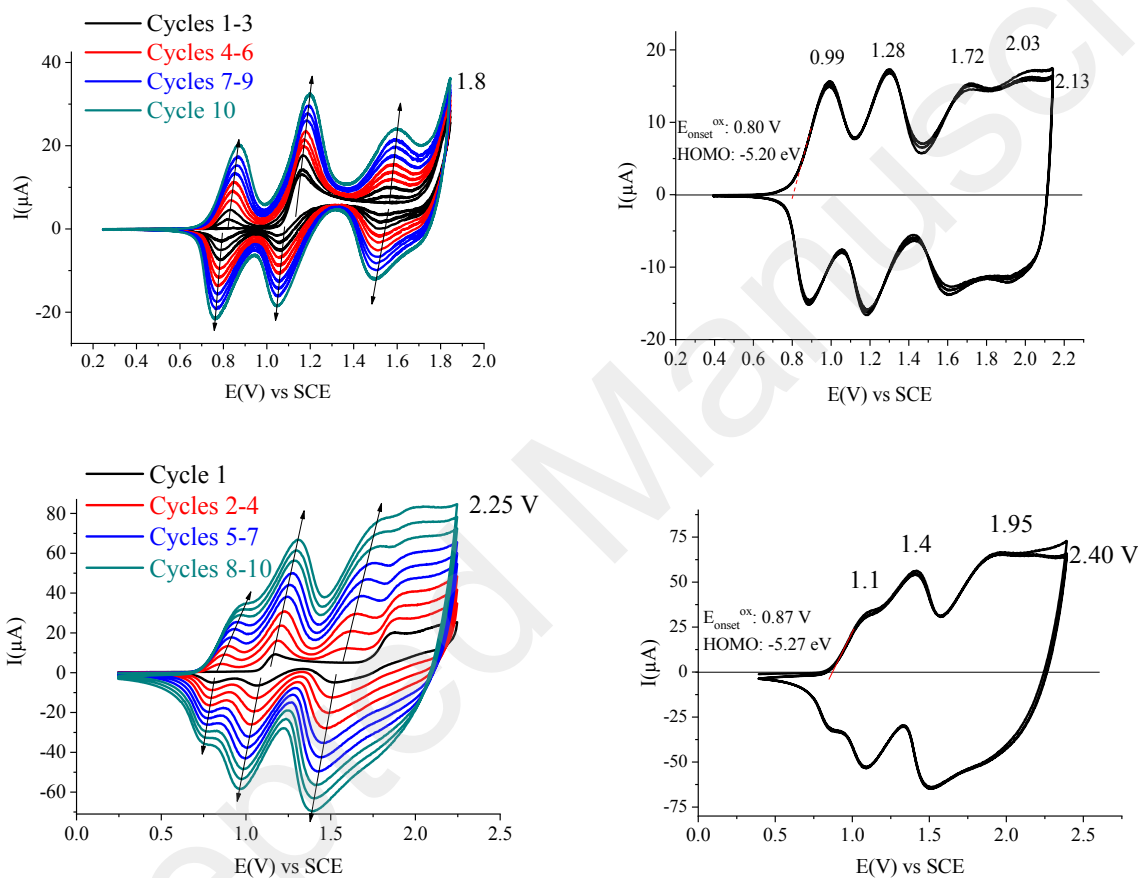


Figure 4. Left: CV (100 mV s^{-1} , $\text{CH}_2\text{Cl}_2/[\text{Bu}_4\text{N}][\text{PF}_6]$ 0.2 M) in the presence of **1-Cbz-SBF**, $2.7 \cdot 10^{-3} \text{ M}$, potential range of the ten successive cycles : 0.2-1.8 V (top) or 0.2-2.25 V (bottom), platinum disk working electrode. Right: CV (100 mV s^{-1} , $\text{CH}_2\text{Cl}_2/[\text{Bu}_4\text{N}][\text{PF}_6]$ 0.2 M) free of any electroactive species, potential limit of the three successive cycles: 0.2-2.13 V (top) or 0.2-2.40 V (bottom), platinum disk working electrode modified by the deposits obtained along the ten cycles in presence of **1-Cbz-SBF**.

After such oxidations, the electrodes are covered with insoluble deposits. Their electrochemical behaviors (recorded in absence of **1-Cbz-SBF**) are presented Figure 4-right. Depending on the potential reached during the electrodeposition, the electrochemical behavior of the corresponding deposits appears somewhat different. When the deposition is performed at low potential (up to 1.80 V), the CV presents four successive redox waves and is stable along recurrent sweeps between

0.60 and 2.13 V. The corresponding HOMO of the deposit is evaluated at -5.20 eV, 0.27 eV higher than that of its corresponding monomer **1-Cbz-SBF**. When the deposition is performed at high potential (up to 2.25 V), the CV is less defined (higher currents are nevertheless reached) displaying only three distinct redox waves weakly shifted compared to those of the previously described deposit. One can note that the HOMO of the polymer is slightly lower, *ie* -5.27 eV, characteristic of a shorter π -conjugation length. For all the deposits, the range of stability is wide showing a high electrochemical stability between 0.50 and 2.40 V.

The electrochemical behavior of deposits prepared during anodic oxidation is presented Figure 5 and compared to that of Poly(Cbz) and Poly(SBF). The deposit obtained from the oxidation of **Cbz** possess the highest HOMO ($E_{\text{onset}}^{\text{ox}}$: 0.57 V, HOMO: -4.97 eV) whereas that of **SBF** the lowest ($E_{\text{onset}}^{\text{ox}}$: 1.10 V, HOMO: -5.50 eV), translating very different π -conjugation pathways between the polymers (Figure 5). In between, begins the p-doping process of the deposit derived from **1-Cbz-SBF** ($E_{\text{onset}}^{\text{ox}}$: 0.87 V, HOMO: -5.27 eV). Such a behavior confirms that carbon-carbon couplings leading to the electrodeposition process of **1-Cbz-SBF** involve both the carbazolyl and the fluorenyl units. The nature of the deposit is however difficult to precisely determinate because at least six carbon atoms may be involved in bonds formation (2 carbon atoms in *para* positions of the nitrogen atom for carbazole and 2 carbon atoms in *para* positions of the biphenyl linkage for both fluorenes).

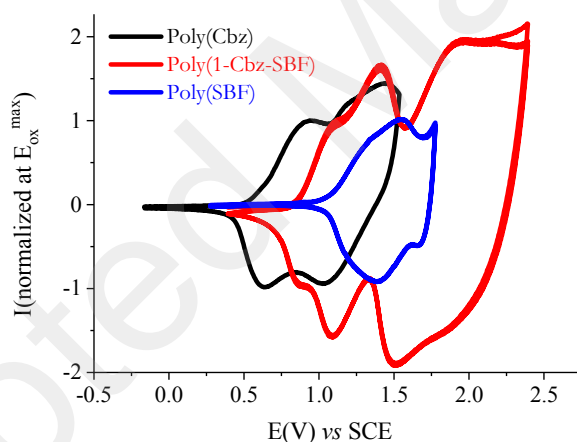


Figure 5. CV (100 mV s^{-1} , $\text{CH}_2\text{Cl}_2/[\text{Bu}_4\text{N}][\text{PF}_6] 0.2 \text{ M}$) free of any electroactive species, platinum disk working electrode modified by: poly(**1-Cbz-SBF**) (red line), anodic limit 2.4 V, poly(**Cbz**) (black line), anodic limit: 2.13 V or poly(**SBF**) (blue line), anodic limit 1.76 V.

Table 1. Selected electronic data of **1-Cbz-SBF**, **SBF** and **Cbz**

	1-Cbz-SBF	SBF ¹	Cbz
HOMO (eV) ^a	-5.47	-5.95	-5.50
Potential of peak oxidation (V) ^b	1.17, 1.87, 2.25	1.67, 1.86	1.18
λ_{abs} (nm) ^c	310, 323, 338	308	319, 332
λ_{em} (nm) ^c	345, 357	310, 323, 340 (sh)	332, 346, 361 (sh)
$\phi^{c,d}$	0.39	0.40	0.25
τ (ns) ^{c,e}	8.1	4.6	7.7
k_{nr} (s ⁻¹) ^c	7.5×10^7	13.0×10^7	9.7×10^7
k_{r} (s ⁻¹) ^c	4.8×10^7	8.7×10^7	3.3×10^7
λ_{T} (nm) ^f	438, 467, 501	431, 463, 490, 500	406
E_{T} (eV) ^f	2.84	2.88	3.05
τ (s) ^f	5.0	5.3	7.4

a: from electrochemical data, b: vs SCE, c: in cyclohexane, d: referenced to quinine sulfate, e: $\lambda_{\text{exc}}=310$ nm, f: 2-MeTHF at 77 K

Optical properties. The UV–vis absorption spectra of **1-Cbz-SBF** and of the two building units **SBF** and **Cbz** recorded in cyclohexane are presented Figure 6 (left). The absorption spectrum of **1-Cbz-SBF** is well structured and displays three main bands at 338, 323 and 310 nm. The band at 338 nm (modelized at $\lambda_{\text{th}} = 287$ nm, see Figure 7) is red shifted by 6 nm compared to that of **Cbz** ($\lambda_{\text{exp}} = 332$ nm, modelized at $\lambda_{\text{th}} = 285$ nm) and possesses a higher molar absorption coefficient (4.3×10^3 L.mol⁻¹.cm⁻¹ for **1-Cbz-SBF** vs 3×10^3 L.mol⁻¹.cm⁻¹ for **Cbz**, Figure 6). In **1-Cbz-SBF**, this band is due to a transition involving two contributions: HOMO→LUMO+3 (56%) and HOMO→LUMO+1 (28%). For the first contribution (HOMO→LUMO+3), molecular orbitals are both localized on the carbazole and for the second contribution (HOMO→LUMO+1) the HOMO is spread out on the carbazole whereas the LUMO+1 is located on the cofacial fluorene (Figure 7). The HOMO→LUMO transition of **Cbz** ($\lambda_{\text{th}}=285$ nm) involves orbitals with the same shape than the first contribution of the first transition in **1-Cbz-SBF**. Therefore, this first contribution can be fully assigned to the carbazole fragment. The second contribution (HOMO→LUMO+1) involving a through space transfer from carbazole to fluorene can explain both the red shift and the higher molar absorption coefficient of **1-Cbz-SBF** compared to **Cbz**. The second band of **1-Cbz-SBF** is

experimentally found at 324 nm ($\lambda_{th}=264$ nm) and possesses a molar absorption coefficient of 3.5×10^3 L.mol⁻¹.cm⁻¹. This band is similar to that found in **Cbz** at 319 nm ($\epsilon=3.5 \times 10^3$ L.mol⁻¹.cm⁻¹, $\lambda_{th}=264$ nm) and is mainly due to a $\pi-\pi^*$ transition involving orbitals localized on the carbazole fragment (major contributions: HOMO-1 \rightarrow LUMO+3 for **1-Cbz-SBF** and HOMO-1 \rightarrow LUMO for **Cbz**). The third band is experimentally found at 311 nm ($\lambda_{th}=271$ nm) and possesses a molar absorption coefficient of 1.2×10^4 L.mol⁻¹.cm⁻¹. This band, which is also found in **SBF** at 308 nm ($\epsilon=1.4 \times 10^3$ L.mol⁻¹.cm⁻¹, $\lambda_{th}=268$ nm)¹ has been assigned to a $\pi-\pi^*$ transition having two contributions: HOMO-2 \rightarrow LUMO (46%) and HOMO-3 \rightarrow LUMO (30%), the three molecular orbitals involved being localized on the SBF fragment. One can indeed note that there is a small red shift of 3 nm between **1-Cbz-SBF** and **SBF** (which is also found in theoretical calculations: $\lambda=271$ and 268 nm respectively) which can be assigned to an alteration of the spiroconjugation (conjugation between the two spiro connected fluorenes)⁶¹⁻⁶⁵ probably due to the particular cofacial arrangement.

In the light of TD-DFT analyses, it is finally important to mention that the HOMO \rightarrow LUMO contribution is involved in two transitions ($\lambda_{th}=272$ and 271 nm) having small oscillator strengths (0.0009 and 0.008). Indeed, as exposed in the electrochemical part, the position 1 induces a π -conjugation breaking between the fluorene and the carbazole leading to the complete spatial separation of HOMO (spread out on the carbazole) and LUMO (spread out on the substituted fluorene). This HOMO \rightarrow LUMO transition is hence strongly disfavored in accordance with a through space electron transfer.^{35, 66-67} To conclude, the absorption spectrum of **1-Cbz-SBF** displays the characteristics of each building block, *ie* **SBF** and **Cbz** but the red shift of the low energy band translates the interactions between the two cofacial units.

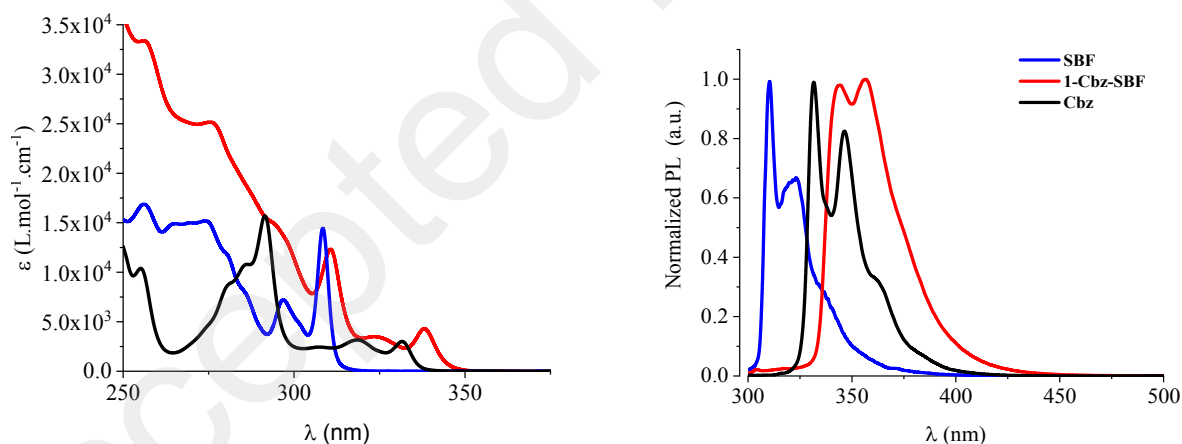


Figure 6. Absorption spectra (left) and normalized emission spectra (right) of **1-Cbz-SBF** (red line), **SBF** (blue line) and **Cbz** (black line) in cyclohexane at room temperature.

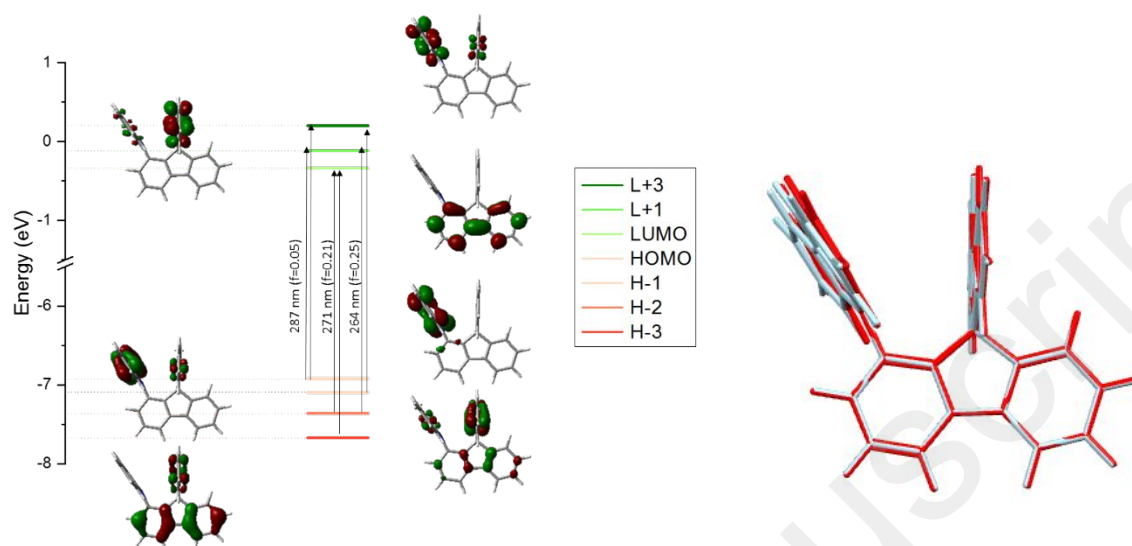


Figure 7. Left: Representation of the energy levels and the main molecular orbitals involved in the electronic transitions of **1-Cbz-SBF** obtained by TD-DFT CAM-B3LYP/6-311+G(d,p), shown with an isovalue of 0.04 [$e \text{ bohr}^{-3}$]^{1/2}. For clarity purposes, only the major contributions (>10%) of each transition is shown (see SI for details). Right: Superposition of optimized geometries of S_0 (ground state, light blue) and S_1 (first singlet excited state, red).

The fluorescence spectrum of **1-Cbz-SBF** presents two maxima at 344 and 357 nm (Figure 6 right). This violet emission is significantly red shifted compared to both **SBF** and **Cbz** showing the impact of the cofacial arrangement on the emission properties. Thus, despite a π -conjugation disruption between the carbazole and SBF fragments, the intramolecular interaction of **1-Cbz-SBF** induces a red shift of the fluorescence spectrum (as commonly observed when there is an electronic coupling between two π -systems) compared to its two constituted fragments. The superposition of the optimized geometries of ground state S_0 and first singlet excited state S_1 (obtained by TD-DFT b3lyp using 6-31g(d) basis set, see SI) shows that there is only a slight difference between these two states. This allows to conclude that the cofacial arrangement in **1-Cbz-SBF** has a key role in its fluorescence, by avoiding strong molecular rearrangements between S_0 and S_1 (Figure 7-Right). We also suggest that the red shift in fluorescence arises from the cofacial arrangement (and not from a more intense electronic coupling in S_1) since the angles between the carbazole and the substituted fluorene planes are the same in S_0 and S_1 (90°). The structured fluorescence spectrum and the small Stokes shift (7 nm) of **1-Cbz-SBF** can also be explained by this very weak reorganization between S_0 and S_1 . This is a different behavior to those previously reported for 2- and 4-substituted SBFs but similar to **1-Ph-SBF** and therefore a characteristic of 1-substituted SBFs family.^{6,23} The fluorescence decays were successfully fitted by single exponentials (See SI), indicating a unique radiative pathway from S_1 to S_0 . The lifetime of **1-Cbz-SBF** ($\lambda_{\text{exc}} = 310 \text{ nm}$, Figure S16) is recorded at 8.1 ns, longer than the lifetimes of **SBF** (4.6 ns)¹ and **Cbz** (7.7 ns, Figure S17), showing once again that the fluorescence of **1-Cbz-SBF** is not the superposition of the emission of **Cbz** and **SBF** but comes from a single fluorophore. Finally, the quantum yield ϕ of **1-Cbz-SBF** was calculated in solution at 0.39 and is identical to that of **SBF** (0.40)¹ and higher than

the one of **Cbz** (0.25). As the non-radiative constant of **1-Cbz-SBF** ($k_{nr} = 7.5 \times 10^7 \text{ s}^{-1}$) is smaller than those of the fragments **SBF** and **Cbz** (resp. $k_{nr} = 13.0 \times 10^7 \text{ s}^{-1}$ and $9.7 \times 10^7 \text{ s}^{-1}$), one can conclude that the internal conversion processes are limited for **1-Cbz-SBF** compared to both **SBF** and **Cbz**.

At this stage, it seems relevant to compare the photophysical data of **1-Cbz-SBF** to those of **1-Ph-SBF** in order to analyze the impact of the C1-substituted SBF scaffold on the photophysical data. The first difference is linked to the quantum yield, which is around 2/3 lower for **1-Cbz-SBF** (0.39) than for **1-Ph-SBF** (0.60). As the non-radiative constants are almost identical for both **1-Cbz-SBF** and **1-Ph-SBF** ($k_{nr} = 7.5 \times 10^7 \text{ s}^{-1}$ and $7.2 \times 10^7 \text{ s}^{-1}$ respectively), one can conclude that the efficiency of the internal conversion processes is similar in the two molecules. Therefore, the lower quantum of **1-Cbz-SBF** finds its origin in the radiative constant k_r which is much lower for **1-Cbz-SBF** ($4.8 \times 10^7 \text{ s}^{-1}$) compared to that of **1-Ph-SBF** ($1.22 \times 10^8 \text{ s}^{-1}$). The loss of quantum yield of **1-Cbz-SBF** is therefore due to a lower electronic transition moment. From a molecular point of view, this feature can be assigned to the carbazole itself and not to the 1-substituted-SBF scaffold (in other words the substitution pattern) as both **SBF** and **1-Ph-SBF** possesses almost identical k_r/k_{nr} .

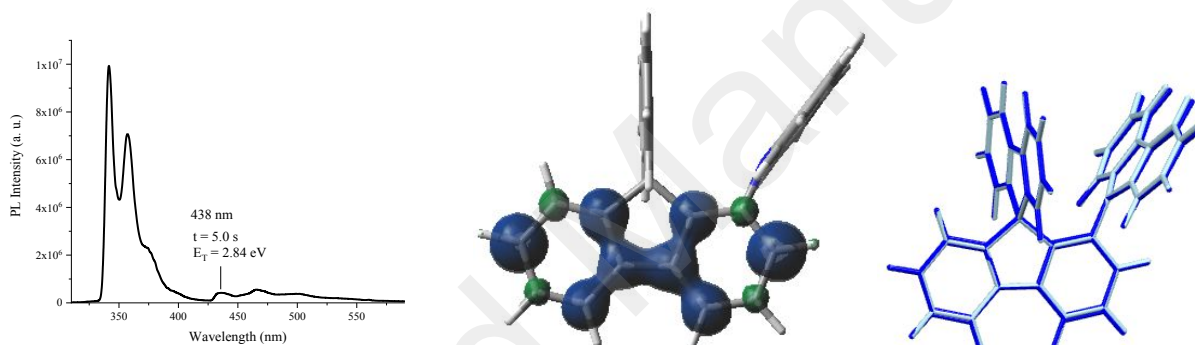


Figure 8. Left: emission spectrum of **1-Cbz-SBF** at 77 K (2-Me-THF, $\lambda_{exc} = 300 \text{ nm}$). Middle: Spin density of triplet of **1-Cbz-SBF** (isovalue= 0.004). Right: Superposition of optimized geometries: S_0 (ground state, light blue) and T_1 (first triplet excited state, blue)

Finally, at 77 K, the emission spectrum of **1-Cbz-SBF** presents a phosphorescence contribution, with a first band centered at 438 nm followed by two other at 467 and 501 nm leading to a very high E_T of 2.84 eV (Figure 8, left). An important feature needs to be stressed out. Indeed, the E_T of **1-Cbz-SBF** is almost identical to that of **SBF** evaluated at 2.88 eV¹ (and smaller than that of **Cbz**, 3.05 eV, measured and determined in identical conditions, Figure S18) highlighting that the pendant substituent has a very weak influence on the T_1 state being hence different to that of S_1 (red shift for **1-Cbz-SBF** compared to **SBF** observed both in absorption and in emission, see above). The high E_T of **1-Cbz-SBF** can be explained by the localization of the triplet exciton, which is exclusively spread out on the substituted fluorene with no contribution of the pendant substituent nor its cofacial fluorene (Figure 8, middle). Therefore, the position C1 which combines an electronic decoupling thanks to the *meta* linkage and a strong steric hindrance seems to be an ideal position to keep a very high E_T . As the potential applications of C1-linked SBFs are in the field of host materials for PhOLEDs, this feature appears promising. In addition, superposition of optimized geometries of the ground state S_0 and the first triplet excited state T_1 shows that the high rigidity of the 1-SBF scaffold strongly prevents reorganization at the first triplet excited state. As

for S_0 , the carbazole-fluorene dihedral angle is very high (90°) at T_1 maintaining the π -conjugation breaking between the two fragments. The E_T decrease of **1-Cbz-SBF** compared to **SBF** can then be assigned to the cofacial arrangement of the 1-substituted SBF scaffold. Radiative deactivation of the triplet state of **1-Cbz-SBF** appears to be very slow under these experimental conditions: ~ 5.0 s. This phosphorescence lifetime is slightly lower compare to that of **SBF** previously reported, 5.3 s¹ (and smaller than that of **Cbz**, 7.4 s) in accordance with a triplet exciton localized on the fluorene. This highlights that the substitution at C1 only slightly modifies the phosphorescent lifetime of the T_1 state.

Conclusions

The present work reports the synthesis and the study of an example of a new emerging family of spirobifluorene based OSCs, namely 1-substituted spirobifluorenes. Thanks to a structure-property relationship study of 1-carbazolyl-spirobifluorene **1-Cbz-SBF** with its building blocks (**SBF** and **Cbz**) and structurally related compounds (**N-Ph-Cbz** and **1-Ph-SBF**) we show that i) there is a complete π -conjugation breaking between the SBF fragment and the pending substituent at C1, and ii) there is an intramolecular interaction between the pending substituent at C1 and the cofacial fluorene (both in solution and in the solid state). The conjugation disruption allows to tune the HOMO energy level of **1-Cbz-SBF**. Indeed, the electronic density is mainly spread out on the pending carbazole leading to a strong increase (by ca 0.5 eV) of the HOMO energy of **1-Cbz-SBF**, -5.47 eV, compared to **SBF**, -5.96 eV. Interestingly, the E_T of **1-Cbz-SBF** is nevertheless maintained at a very high value (2.84 eV) almost identical to that of **SBF**, 2.88 eV. Thus, some electronic properties are driven by the pending carbazole whereas others by the SBF fragment. Furthermore, the strong carbazole/fluorene through space interaction modifies some electronic properties (red shift of the absorption and fluorescence spectra), keeping other almost unaltered (phosphorescence). This π - π interaction between the C1-linked substituent and the cofacial fluorene is therefore an interesting tool to modulate the electronic properties of SBF based materials. In the light of the development of new generations of SBF regioisomers in the last ten years, we believe that 1-substituted SBFs constitute an interesting platform for future organic materials in OE, notably as hosts for PhOLEDs. We are currently working in this direction.

Supporting Information Available

General Experimental Methods, synthesis and characterization, details on NMR, electrochemical and photophysical studies, X-Ray and theoretical modelling. Copy of NMR spectra.

Abbreviations

PhOLED, phosphorescent organic light-emitting diode; HOMO, highest occupied molecular orbital; LUMO, lowest unoccupied molecular orbital; SBF, 9,9'-spirobifluorene; OSC, organic semi-conductor; OE, Organic Electronics; OLED, organic light emitting diode; E_T , triplet state energy; TMEDA, N,N,N',N'-tetramethylethylenediamine; NMR, nuclear magnetic resonance; CV, cyclic voltammetry; DPV, differential pulse voltammetry; TD-DFT, time-dependent density functional theory; THF, tetrahydrofuran; HFIP, Hexafluoro-2-propanol; TFA, trifluoroacetic acid; SCE, saturated calomel electrode.

Conflicts of interest

There are no conflicts to declare.

Acknowledgments

The authors would like to thank the CINES (Montpellier N° 2018-A0040805032) for computing time, S. Thiery for preliminary works on 1-carbazolyl-fluorenone and the ANR (n°14-CE05-0024) for a PhD grant (LJS) and a post-doctoral position (CQ) and for financial support.

References

1. Sicard, L.; Quinton, C.; Peltier, J.-D.; Tondelier, D.; Geffroy, B.; Biapo, U.; Métivier, R.; Jeannin, O.; Rault-Berthelot, J.; Poriel, C., Spirobifluorene regioisomerism *Chem. Eur. J.* **2017**, *23*, 7719-7723.
2. Poriel, C.; Rault-Berthelot, J., Structure–property relationship of 4-substituted-spirobifluorenes as hosts for phosphorescent organic light emitting diodes: an overview. *J. Mater. Chem. C* **2017**, *5*, 3869-3897
3. Saragi, T. P. I.; Spehr, T.; Siebert, A.; Fuhrmann-Lieker, T.; Salbeck, J., Spiro compounds for organic optoelectronics. *Chem. Rev.* **2007**, *107*, 1011-1065.
4. Ma, Z.; Sonar, P.; Chen, Z.-K., Recent progress in fluorescent blue materials. *Current Organic Chemistry* **2010**, *18*, 2039-2069.
5. Poriel, C.; Rault-Berthelot, J., Dihydroindenofluorene positional isomers. *Acc. Chem. Res.* **2018**, *51*, 1818-1830.
6. Quinton, C.; Thiery, S.; Jeannin, O.; Tondelier, D.; Geffroy, B.; Jacques, E.; Rault-Berthelot, J.; Poriel, C., Electron-rich 4-substituted spirobifluorenes: Toward a new Family of high triplet energy host materials for high-efficiency green and sky blue phosphorescent OLEDs *ACS Appl. Mater. Interfaces.* **2017**, *9*, 6194-6206.
7. Wong, K.-T.; Liao, Y.-L.; Lin, Y.-T.; Su, H.-C.; Wu, C.-C., Spiro-configured bifluorenes: Highly efficient emitter for UV organic light-emitting device and host material for red electrophosphorescence *Org. Lett.* **2005**, *7*, 5131-5134.
8. Xing, X.; Xiao, L.; Zheng, L.; Hu, S.; Chen, Z.; Qu, B.; Gong, Q., Spirobifluorene derivative: a pure blue emitter (CIE $y \approx 0.08$) with high efficiency and thermal stability *J. Mater. Chem.* **2012**, *22*, 15136-15140.
9. Lee, H.; Jung, H.; Kang, S.; Heo, J. H.; Im, S. H.; Park, J., Three-dimensional structures based on the fusion of chrysene and spirobifluorene chromophores for the development of blue OLEDs- high performance in non-doped blue oled. *J. Org. Chem* **2018**, *83*, 2640-2646.
10. Zhu, M.; Yang, C., Blue fluorescent emitters: design tactics and applications in organic light-emitting diodes *Chem. Soc. Rev.* **2013**, *42*, 4963-4976.
11. Tang, S.; Liu, M.; Lu, P.; Xia, H.; Li, M.; Xie, Z.; Shen, F. Z.; Gu, C.; Wang, H.; Yang, B. et al, A molecular glass for deep-blue organic light-emitting diodes comprising a 9,9'-spirobifluorene core and peripheral carbazole groups *Adv. Funct. Mat.* **2007**, *17*, 2869-2877.

- 1
2
3
4
5
6
7
8
9
10
11
12
13
14
15
16
17
18
19
20
21
22
23
24
25
26
27
28
29
30
31
32
33
34
35
36
37
38
39
40
41
42
43
44
45
46
47
48
49
50
51
52
53
54
55
56
57
58
59
60
12. Wei, Y.; Chen, C.-T., Doubly ortho-linked cis-4,4'-bis(diarylamino)stilbene/fluorene hybrids as efficient non-doped sky-blue fluorescent materials for optoelectronic applications *J. Am. Chem. Soc.* **2007**, *129*, 7478-7479.
 13. Bian, M.; Wang, Y.; Guo, X.; Lv, F.; Chen, Z.; Duan, L.; Bian, Z.; Liu, Z.; Geng, H.; Xiao, L., Positional isomerism effect of spirobifluorene and terpyridine moieties of "(A)_n-D-(A)_n" type electron transport materials for long-lived and highly efficient TADF-PhOLEDs. *J. Mater. Chem. C* **2018**, *6*, 10276-10283.
 14. Shen, J. Y.; Lee, C. Y.; Huang, T.-H.; Lin, J. T.; Tao, Y.-T.; Chen, C.-H.; Tsai, C., High T_g blue emitting materials for electroluminescent devices *J. Mater. Chem.* **2005**, *15*, 2455-2463.
 15. Li, G.; Wang, S.; Liu, T.; Hao, P.; Liu, Z.; Li, F.; Yang, L.-M.; Zhang, Y.; Li, D.; Yang, S.; et al, Non-fullerene acceptor engineering with three-dimensional thiophene/selenophene-annulated perylene diimides for high performance polymer solar cells. *J. Mater. Chem. C* **2018**, *6*, 12601-12607.
 16. Li, S.; Liu, W.; Shi, M.; Mai, J.; Lau, T.-K.; Wan, J.; Lu, X.; Li, C.-Z.; Chen, H., A spirobifluorene and diketopyrrolopyrrole moieties based non-fullerene acceptor for efficient and thermally stable polymer solar cells with high open-circuit voltage. *Energy Environ. Sci* **2016**, *9*, 604-610.
 17. Xia, D.; Gehrig, D.; Guo, X.; Baumgarten, M.; Laquai, F.; Mullen, K., A spiro-bifluorene based 3D electron acceptor with dicyanovinylene substitution for solution-processed non-fullerene organic solar cells. *J. Mater. Chem. A* **2015**, *3*, 11086-11092.
 18. Yi, J.; Wang, Y.; Luo, Q.; Lin, Y.; Tan, H.; Wang, H.; Ma, C.-Q., A 9,9'-spirobi[9H-fluorene]-cored perylenediimide derivative and its application in organic solar cells as a non-fullerene acceptor. *Chem. Commun.* **2016**, *52*, 1649-1652.
 19. Wu, X.-F.; Fu, W.-F.; Xu, Z.; Shi, M.; Liu, F.; Chen, H.-Z.; Wan, J.-H.; Russell, T. P., Spiro linkage as an alternative strategy for promising non-fullerene acceptors in organic solar cells. *Adv. Funct. Mat.* **2015**, *25*, 5954-5966.
 20. Sicard, L. J.; Li, H.-C.; Wang, Q.; Liu, X.-Y.; Jeannin, O.; Rault-Berthelot, J.; Liao, L.-S.; Jiang, Z.-Q.; Poriel, C., C1-Linked spirobifluorene dimers: pure hydrocarbon hosts for high-performance blue phosphorescent OLEDs. *Angew. Chem. Int. Ed.* **2019**, *58*, 3848-3853.
 21. Jiang, Z.; Yao, H.; Zhang, Z.; Yang, C.; Liu, Z.; Tao, Y.; Qin, J.; Ma, D., Novel oligo-9,9'-spirobifluorenes through ortho-linkage as full hydrocarbon host for highly efficient phosphorescent OLEDs *Org. Lett.* **2009**, *11*, 2607-2610.
 22. Cui, L.-S.; Dong, S.-C.; Liu, Y.; Xu, M.-F.; Li, Q.; Jiang, Z.-Q.; Liao, L.-S., Meta-Linked spirobifluorene/phosphine oxide hybrids as host materials for deep blue phosphorescent organic light-emitting diodes. *Org. Electron.* **2013**, *14*, 1924-1930.
 23. Thiery, S.; Declairieux, C.; Tondelier, D.; Seo, G.; Geffroy, B.; Jeannin, O.; Métivier, R.; Rault-Berthelot, J.; Poriel, C., 2-Substituted vs 4-substituted-9,9'-spirobifluorene host materials for green and blue phosphorescent OLEDs: a structure-property relationship study *Tetrahedron* **2014**, *70*, 6337-6351

- 1
2
3 24. Thiery, S.; Tondelier, D.; Declairieux, C.; Geffroy, B.; Jeannin, O.; Métivier, R.; Rault-
4 Berthelot, J.; Poriel, C., 4-Pyridyl-9,9'-spirobifluorenes as host materials for green and sky-blue
5 phosphorescent OLEDs *J. Phys. Chem. C* **2015**, *119*, 5790-5805
6
7 25. Bulut, I.; Chavez, P.; Fall, S.; Mery, S.; Heinrich, B.; Rault-Berthelot, J.; Poriel, C.;
8 Leveque, P.; Leclerc, N., Incorporation of spirobifluorene regioisomers in electron-donating
9 molecular systems for organic solar cells. *RSC Adv.* **2016**, *6*, 25952-25959
10
11 26. Dong, S.-C.; Gao, C.-H.; Zhang, Z.-H.; Jiang, Z.-Q.; Lee, S.-T.; Liao, L. S., New
12 dibenzofuran/spirobifluorene hybrids as thermally stable host materials for efficient
13 phosphorescent organic light-emitting diodes with low efficiency roll-off *Phys. Chem. Chem.*
14 *Phys.* **2012**, *14*, 14224-14228.
15
16 27. Dong, S.-C.; Gao, C.-H.; Yuan, X. D.; Cui, L.-S.; Jiang, Z.-Q.; Lee, S.-T.; Liao, L. S.,
17 Novel dibenzothiophene based host materials incorporating spirobifluorene for high-efficiency
18 white phosphorescent organic light-emitting diodes *Org. Electron.* **2013**, *14*, 902-908.
19
20 28. Lee, K. H.; Kim, S. O.; Yook, K. S.; Jeon, S. O.; Lee, J. Y.; Yoon, S. S., Highly efficient
21 blue light-emitting diodes containing spirofluorene derivatives end-capped with
22 triphenylamine/phenylcarbazole *Synth. Met.* **2011**, *161*, 2024-2030.
23
24 29. Liu, Y.; Cui, L.-S.; Shi, X.-B.; Li, Q.; Jiang, Z.-Q.; Liao, L.-S., Improved host material for
25 electrophosphorescence by positional engineering of spirobifluorene-carbazole hybrids *J. Mater.*
26 *Chem. C* **2014**, *2*, 8736-8744.
27
28 30. Ding, L.; Du, S.; Cui, L.-S.; Zhang, F.-H.; Liao, L.-S., Novel spiro-based host materials for
29 application in blue and white phosphorescent organic light-emitting diodes *Org. Electron.* **2016**,
30 *37*, 108-114.
31
32 31. Kharasch, N.; Bruce, T. C., Derivatives of sulfenic acids. V. 1-fluorenone sulfur
33 compounds *J. Am. Chem. Soc.* **1951**, *73*, 3240-3244.
34
35 32. George, S. R. D.; Scott, L. T.; Harper, J. B., Synthesis of 1-substituted fluorenones.
36 *Polycyclic Aromatic Compounds* **2016**, *36*, 697-715.
37
38 33. Chen, X.-Y.; Ozturk, S.; Sorensen, E. J., Synthesis of fluorenones from benzaldehydes and
39 aryl iodides: Dual C-H functionalizations using a transient directing group. *Org. Lett.* **2017**, *19*,
40 1140-1143.
41
42 34. Hedidi, M.; Erb, W.; Lassagne, F.; Halauko, Y. S.; Ivashkevich, O. A.; Matulis, V. E.;
43 Roisnel, T.; Bentabed-Ababsa, G.; Mongin, F., Functionalization of pyridyl ketones using
44 deprotonation-in situ zincation. *RSC Advances* **2016**, *6*, 63185-63189.
45
46 35. Romain, M.; Tondelier, D.; Jeannin, O.; Geffroy, B.; Rault-Berthelot, J.; Poriel, C., D
47 Properties modulation of organic semi-conductors based on a donor-spiro-acceptor (D-spiro-A)
48 molecular design: New host materials for efficient sky-blue PhOLEDs *J. Mater. Chem. C* **2015**,
49 *3*, 97010-97014.
50
51 36. Poriel, C.; Cocherel, N.; Rault-Berthelot, J.; Vignau, L.; Jeannin, O., Incorporation of
52 spiroxanthene units in blue-emitting oligophenylene frameworks: A new molecular design for
53 OLED applications. *Chem. Eur. J.* **2011**, *17*, 12631-12645.
54
55 37. Thiery, S.; Tondelier, D.; Geffroy, B.; Jeannin, O.; Rault-Berthelot, J.; Poriel, C.,
56 Modulation of the physicochemical properties of donor-spiro-acceptor derivatives through donor
57
58
59
60

unit planarisation: Phenylacridine versus indoloacridine-new hosts for green and blue phosphorescent organic light-emitting diodes (PhOLEDs) *Chem. Eur. J.* **2016**, *22*, 10136-10149.

38. Thirion, D.; Poriel, C.; Métivier, R.; Rault-Berthelot, J.; Barrière, F.; Jeannin, O., Violet-to-blue tunable emission of aryl-substituted dispirofluorene–indenofluorene isomers by conformationally-controllable intramolecular excimer formation. *Chem. Eur. J.* **2011**, *17*, 10272-10287.

39. Rathore, R.; Abdelwahed, S. H.; Guzei, I. A., Synthesis, structure, and evaluation of the effect of multiple stacking on the electron-donor properties of π -stacked polyfluorenes *J. Am. Chem. Soc.* **2003**, *125*, 8712-8719.

40. Nakano, T.; Yade, T., Synthesis, structure, and photophysical and electrochemical properties of a π -stacked polymer *J. Am. Chem. Soc.* **2003**, *125*, 15474-15484.

41. Thirion, D.; Poriel, C.; Barrière, F.; Métivier, R.; Jeannin, O.; Rault-Berthelot, J., Tuning the optical properties of aryl-substituted dispirofluorene–indenofluorene isomers through intramolecular excimer formation. *Org. Lett.* **2009**, *11*, 4794-4797.

42. Wang, W.-L.; Xu, J.; Sun, Z.; Zhang, X.; Lu, Y.; Lai, Y.-H., Effect of transannular π – π interaction on emission spectral shift and fluorescence quenching in dithia[3.3]paracyclophane–fluorene copolymers *Macromolecules* **2006**, *39*, 7277-7285.

43. Cornelis, D.; Franz, E.; Asselberghs, I.; Clays, K.; Verbiest, T.; Koeckelberghs, G., Terchromophoric interactions in chiral X-type π -conjugated oligomers: A linear and nonlinear optical study *J. Am. Chem. Soc.* **2011**, *133*, 1317-1322.

44. Nandy, R.; Subramoni, M.; Varghese, B.; Sankararaman, S., Intramolecular π -stacking interaction in a rigid molecular hinge substituted with 1-(pyrenylethynyl) units *J. Org. Chem.* **2007**, *72*, 938-944.

45. Poriel, C.; Rault-Berthelot, J.; Thirion, D.; Barrière, F.; Vignau, L., Blue emitting 3 π –2 Spiro terfluorene–indenofluorene isomers: A structure–properties relationship study. *Chem. Eur. J.* **2011**, *17*, 14031-14046.

46. Bondi, A., van der Waals volumes and radii *J. Phys. Chem.* **1964**, *68*, 441-451.

47. Yang, X.-J.; Drepper, F.; Wu, B.; Sun, W.-H.; Haehnel, W.; Janiak, C., From model compounds to protein binding: syntheses, characterizations and fluorescence studies of [RuII(bipy)(terpy)L]²⁺ complexes (bipy = 2,2'-bipyridine; terpy = 2,2':6',2''-terpyridine; L = imidazole, pyrazole and derivatives, cytochrome c) *Dalton Trans.* **2005**, 256-267.

48. Craven, E.; Zhang, C.; Janiak, C.; Rheinwald, G.; Lang, H., Dimethyl-2,2'-bipyridine)(IDA)copper(II) and structural comparison with aqua(IDA)(1,10-phenanthroline)copper(II) (IDA = iminodiacetato) *Anorg. Allg. Chem* **2003**, *629*, 2282-2290.

49. Janiak, C., A critical account on π – π stacking in metal complexes with aromatic nitrogen-containing ligands *J. Chem. Soc., Dalton Trans.* **2000**, 3885-3896.

50. Banerjee, S.; Ghosh, A.; Wu, B.; Lassahn, P.-G.; Janiak, C. Polymethylene spacer regulated structural divergence in cadmium complexes: Unusual trigonal prismatic and severely distorted octahedral coordination *Polyhedron* **2005**, *24*, 593-599.

- 1
2
3 51. Ambrose, J. F.; Nelson, R. F., Anodic oxidation pathways of carbazoles I . carbazole and
4 N-substituted derivatives *J. Electrochem. Soc.* **1968**, 1159-1164.
5
6 52. Tang, G.-M.; Chi, R.-H.; Wan, W.-Z.; Chen, Z.-Q.; Yan, T.-X.; Dong, Y.-P.; Wang, Y.-
7 T.; Cui, Y.-Z., Tunable photoluminescent materials based on two phenylcarbazole-based dimers
8 through the substituent groups. *J. Lumin.* **2017**, 185, 1-9.
9
10 53. Chebny, V. J.; Shukla, R.; Lindeman, S. V.; Rathore, R., Molecular Actuator: Redox-
11 Controlled Clam-Like Motion in a Bichromophoric Electron Donor *Org. Lett.* **2009**, 11, 1939-
12 1942.
13
14 54. Qi, H.; Chang, J.; Abdelwahed, S. H.; Thakur, K.; Rathore, R.; Bard, A. J.,
15 Electrochemistry and electrogenerated chemiluminescence of π -stacked poly(fluorenemethylene)
16 oligomers. Multiple, interacting electron transfers. *J. Am. Chem. Soc.* **2012**, 134, 16265-16274.
17
18 55. Poriel, C.; Rault-Berthelot, J.; Thirion, D., Modulation of the electronic properties of 3 π -
19 2spiro compounds derived from bridged oligophenylenes: A structure-property relationship. *J.*
20 *Org. Chem.* **2013**, 73, 886-898.
21
22 56. Rault-Berthelot, J.; Granger, M. M.; Mattiello, L., Anodic oxidation of 9,9'-spirobifluorene
23 in CH₂Cl₂+0.2 M Bu₄NBF₄. Electrochemical behaviour of the derived oxidation product. *Synth.*
24 *Met.* **1998**, 97, 211-215.
25
26 57. Poriel, C.; Ferrand, Y.; Le Maux, P.; Rault-Berthelot, J.; Simonneaux, G., Organic cross-
27 linked electropolymers as supported oxidation catalysts: Poly((tetrakis(9,9'-
28 spirobifluorenyl)porphyrin)manganese) films *Inorg. Chem.* **2004**, 43, 5086-5095.
29
30 58. Ferrand, Y.; Poriel, C.; Le Maux, P.; Rault-Berthelot, J.; Simonneaux, G., Asymmetric
31 heterogeneous carbene transfer catalyzed by optically active ruthenium spirobifluorenylporphyrin
32 polymers. *Tetrahedron Asymmetry* **2005**, 16, 1463-1472.
33
34 59. Poriel, C.; Ferrand, Y.; Le Maux, P.; Paul-Roth, C.; Simonneaux, G.; Rault-Berthelot, J.,
35 Anodic oxidation and physicochemical properties of various porphyrin-fluorenes or -
36 spirobifluorenes: Synthesis of new polymers for heterogeneous catalytic reactions *J. Electroanal.*
37 *Chem.* **2005**, 583, 92-103.
38
39 60. Poriel, C.; Ferrand, Y.; Juillard, S.; Le Maux, P.; Simonneaux, G., Synthesis and
40 stereochemical studies of di and tetra 9,9'-spirobifluorene porphyrins: New building blocks for
41 catalytic material *Tetrahedron* **2004**, 60, 145-158.
42
43 61. Geuenich, D.; Hess, K.; Köhler, F.; Herges, R., Anisotropy of the induced current density
44 (ACID), a general method to quantify and visualize electronic delocalization *Chem. Rev.* **2005**,
45 105, 3758-3772.
46
47 62. Simmons, H. E.; Fukunaga, T., Spiroconjugaison. *J. Am. Chem. Soc.* **1967**, 89, 5208.
48
49 63. Hintschich, S. I.; Rothe, C.; King, S. M.; Clark, S. J.; Monkman, A. P., The complex
50 excited-state behavior of a polyspirobifluorene derivative: The role of spiroconjugation and mixed
51 charge transfer character on excited-state stabilization and radiative lifetime *J. Phys. Chem. B*
52 **2008**, 112, 16300-16306.
53
54 64. Lukes, V.; Solc, R.; Milota, F.; Sperling, J.; Kauffmann, H. F., Theoretical investigation of
55 the structure and the electron-vibrational dynamics of 9,9'-spirobifluorene *Chem. Phys.* **2008**, 349,
56 226-233.
57
58
59
60

- 1
2
3 65. Kowada, T.; Kuwabara, T.; Ohe, K., Synthesis, structures, and optical properties of
4 heteroarene-fused dispiro compounds *J. Org. Chem.* **2010**, *75*, 906-913.
5
6 66. Pan, H.; Fu, G.-L.; Zhao, Y.-H.; Zhao, C.-H., Through-space charge-transfer emitting
7 biphenyls containing a boryl and an amino group at the *o,o'*-positions *Org. Lett.* **2011**, *13*, 4830-
8 4833.
9
10 67. Romain, M.; Tondelier, D.; Geffroy, B.; Jeannin, O.; Jacques, E.; Rault-Berthelot, J.;
11 Poriel, C., Donor/Acceptor dihydroindeno[1,2-*a*]fluorene and dihydroindeno[2,1-*b*]fluorene:
12 Towards new families of organic semiconductors. *Chem. Eur. J.* **2015**, *21*, 9426-9439.
13
14
15
16
17
18
19
20
21
22
23
24
25
26
27
28
29
30
31
32
33
34
35
36
37
38
39
40
41
42
43
44
45
46
47
48
49
50
51
52
53
54
55
56
57
58
59
60

TOC GRAPHIC

